Electronic Research Archive

http://www.aimspress.com/journal/era

ERA, 32(2): 812–835.
DOI: 10.3934/era.2024039
Received: 06 November 2023
Revised: 20 December 2023
Accepted: 08 January 2024
Published: 12 January 2024

Research article

The preview control of a corticothalamic model with disturbance

Denggui Fan[1], Yingxin Wang[1], Jiang Wu[1], Songan Hou[2] and Qingyun Wang[2,*]

[1] School of Mathematics and Physics, University of Science and Technology Beijing, Beijing 100083, China

[2] Department of Dynamics and Control, Beihang University, Beijing 100191, China

* **Correspondence:** Email: nmqingyun@163.com.

Abstract: Based on a neural field network model with impulsive and random disturbances, a preview control method that makes full use of known future information is proposed to reduce the static error of the target signal and the transient oscillatory behavior of the controlled system when it receives random disturbance inputs. The preview controller for epileptic seizures is constructed, and the feasibility and effectiveness of clinical single-target and multi-target stimulation in epilepsy regulation are explored from a computational perspective. In addition, a performance index function is proposed to evaluate the energy consumption of controller with and without preview under different input (target) strategies. Suggestions for different strategies are given in terms of the individualized disease environment of patients. From the perspective of seizure control effectiveness and performance consumption, the results show that the preview controller has a greater advantage. The theory of preview control is applied to the control of epileptic seizures for the first time, and the conclusions of the multifaceted study provide some references for clinical trials and controller applications.

Keywords: thalamocortical model; epileptic spike and wave discharges; preview control; linear matrix inequality

1. Introduction

Epilepsy is a neurological disorder characterised by abnormal brain rhythms recorded at the macroscopic level of EEG electrodes typically during seizures [1]. The electrographic epileptiform phenomena in the case of absence seizures, myoclonic seizures and complex partial seizures are often comprised of periodic spike and wave discharges (SWD) in the EEG, which is chacterized by a fast spike followed by a slow wave [2].

Epileptic seizure is fundamentally a dynamic disease [3, 4] which occurs in an intact physiological system. This system operates in a range of control parameters that lead to abnormal dynamics [5–7].

For the detection of seizures, scholars are also exploring new markers [8]. The further clinical challenge is to take into account the evolving dynamics of epilepsy with the goal of developing effective treatment strategies. There is a considerable literature on the possible mechanism of generation of SWD which is ascribed to the most commonly accepted 'cortico-reticular' theory [9], i.e., SWD bursts are generated by an interplay between thalamus and cortex. Thus, the computational challenge is to understand the relationship between the structure of the nervous system and the dynamic abnormalities generated by epileptic neural populations [10, 11].

Investigations showed that a brief sensory or electrical stimulus given at seizure onset can sometimes incur [12, 13], abate [14] or abort [15–17] the seizure events of epilepsy. The mantra of dynamic systems theory is that qualitative changes in dynamics, referred to as bifurcations, occur as an important parameter(s) crosses stability boundaries [18, 19]. In fact, epileptic phenomena are generally modeled by a bistability of silence and seizure-like bursting. It is demonstrated in a bistable model that single pulse perturbations can both induce and abate abnormal epileptiform activity [20, 21]. This approach is to apply single pulse perturbations in state space beyond the manifold which separates the seizure and non-seizure attractor [22, 23]. One of the assumptions of our study is that the background state coexists with the SWD limit cycle in the state space [23].

While there is obvious appeal to single pulse stimulation, there are many difficulties with that approach, especially in stochastic systems where repeated success can be troublesome [22]. In addition, stimulation involves many control parameters such as stimulation cycle, pulse width, intensity and stimulation direction, which are difficult both theoretically and clinically. In contrast, nonlinear feedback controller and observer are designed to suppress the epileptic seizures [24, 25]. Neural Mass Model (NMM) is a biologically inspired model able to reproduce signals observed in spontaneous electroencephalograms (and evoked potentials), and it allows one to apply those controllers.

The control of a system with epileptic SWD oscillations is highly nontrivial since the system is nonlinear [26]. Broadly speaking, optimal control, according to the control theory, is a mathematical framework that allows for the systematic selection of time-varying inputs to effectively drive a dynamical system in a desired way [22, 27]. Optimal control theory has been utilized not just in seizures [27], but also in the studies of other disease models, including the SIR Model of infectious illnesses [28, 29] and the complication Type 2 diabetes [30]. However, for epileptic seizures, the nonlinear controller designed in the previous literature can effectively control it [20, 27], they do not consider how to effectively eliminate or suppress random disturbances. From this perspective, we try to utilize the theory of preview control to attenuate or eliminate the effects of random disturbances on the epileptic system. Preview control can make full use of the known future information to reduce the static error and to improve the performance of inhibiting transient responses [31–34]. Optimizing the utilization of the known future reference signals or disturbance signals to improve the control performance of epileptic seizure system continues to be a significant area of research.

Indeed, in addition to impulse stimulation, the random disturbance (real brain environmental noise or other external stimulation interference) has been theoretically demonstrated to induce epileptic seizures and further propagation due to the mechanisms of bistability or excitability [4]. That is, when the controlled system receives the disturbance again, a transient oscillation may be induced, which as the disturbance input may also induce the seizure of the other adjacent coupled nodes. This might be an issue that almost all controller designs ignore.

We conduct the first study attempting to use preview controllers to control epileptic seizures. We explore whether the preview controller can stabilize the controlled system (the current system) after a second disturbance. Therefore, our contributions and innovations are as follows:

• In this study, based on a computational model of epileptic spike-wave dynamics with disturbances, we aim to design a preview controller that is capable of suppressing epileptic seizures after receiving impulsive and noisy disturbances. We compare the control effect of the preview controllers and non-preview controllers, and the results show that the preview controllers have better effect.

• In particular, we consider single-input and multi-input cooperative control strategies to explore the feasibility and effectiveness of clinical multi-target stimulation in epilepsy regulation from a computational perspective. By discussing the control strategies of various nuclei, we aim to explore the strategies that can make the system oscillate less or even not oscillate after secondary disturbance. This research serves as a point of reference for clinical epilepsy regulation.

• In addition, we propose a cost performance function for evaluating the energy consumption of preview control and non-preview control under different input control strategies. The lower performance consumption can extend the operating time of controllers. Comparing the consumption of different strategies, we discuss controller strategies with better performance and lower consumption.

2. Dynamics of the corticothalamic model

2.1. The corticothalamic model generating generalized spike and wave discharges (SWD) of idiopathic generalized epilepsy (IGE)

Considerable literatures showed that SWD are generated by an interplay between the thalamus and cortex [35–37] by which normal thalamic discharges are sent to a slightly hyperexcitable cortex, which responds with spike and wave activity. Mathematical models of neural field dynamics provide a safer way to explore the effect of brain stimulations than in vivo experimentation. Several models of SWD have been proposed in literature to study mechanisms of SWD seizure genesis and dynamics [38–40].

Neural population models describe the macroscopic neural activity that can be clinically recorded by an electroencephalogram (EEG) (see Figure 1(a)). Since most patient data is collected by EEG, which operates at the macroscopic scale, similar to the previous work, in this work we propose a clinically relevant thalamocortical circuit neural population model with random disturbance.

The original model from the work [27] and used in this paper is given as follows:

$$\begin{cases} \dot{PY}(t) = \tau_1(h_{py} - PY + C_1 S[PY] - C_3 S[IN] + C_9 S[TC]), \\ \dot{IN}(t) = \tau_2(h_{in} - IN + C_2 S[PY]), \\ \dot{TC}(t) = \tau_3(h_{tc} - TC - C_6 L[RE] + C_7 S[PY]), \\ \dot{RE}(t) = \tau_4(h_{re} - RE - C_4 L[RE] + C_5 L[TC] + C_8 S[PY]). \end{cases} \tag{2.1}$$

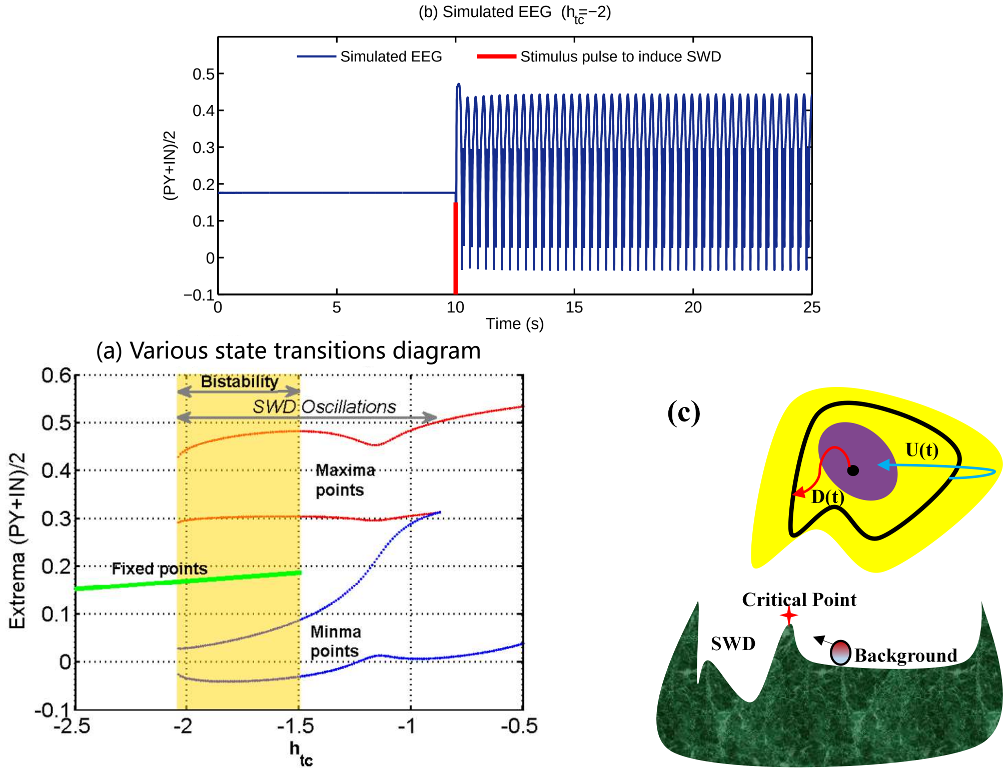

Figure 1. (a) Various state transitions diagram. Minima and maxima of time series for different values of h_{tc}. (b) Time series of the model output. (c) Schematic for the bistability between SWD (black line) and background (black dot) state attractors, where yellow and purple regions are their domain of attraction, respectively. The red cross represents the critical point between different states, and ball represents the system. $U(t)$ is the control input or abatement perturbation, where $D(t)$ is the disturbance inducing seizures.

As seen from Figure 2, the cortical subsystem is composed of excitatory pyramidal (PY) and inhibitory interneuron (IN) populations. The thalamic subsystem includes variables representing populations of thalmocortical relay cells (TC) and neurons located in the reticular nucleus (RE).

All populations are interconnected in agreement with experimentally known connections using the connectivity parameters $C_i(i = 1, 2, ...9)$. $h_{py}, h_{in}, h_{tc}, h_{re}$ are input parameters, $\tau_1, \tau_2, \tau_3, \tau_4$ are timescale parameters, and $C_1 = 1.8, C_2 = 4, C_3 = 1.5, C_4 = 0.2, C_5 = 10.5, C_6 = 0.6, C_7 = 3, C_8 = 3, C_9 = 1, h_{py} = -0.35, h_{in} = -3.4, h_{tc} = -2, h_{re} = -5, \tau_1 = 26, \tau_2 = 1.25 \times 26, \tau_3 = 0.1 \times 26, \tau_4 = 0.1 \times 26$. $S(x)$ is the sigmoid function:

$$S(x) = 1/(1 + \epsilon^{-x}), \tag{2.2}$$

$L(x)$ is the linear function:

$$L(x) = ax + b, \tag{2.3}$$

and $\epsilon = 250,000, a = 2.8, b = 0.5$.

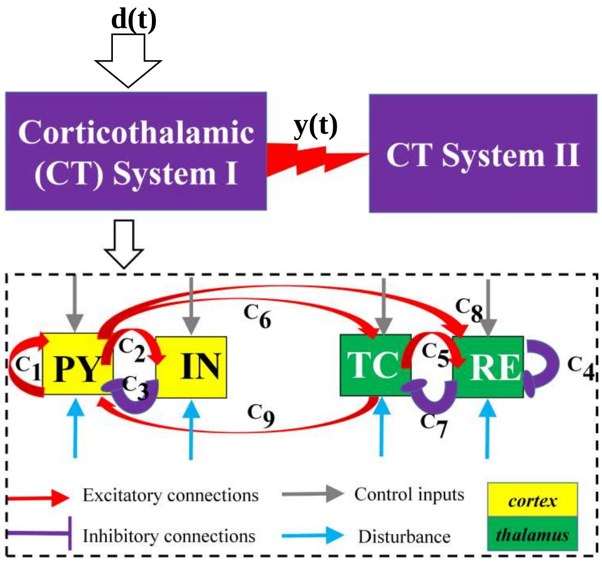

Figure 2. Schematics of two separate corticothalamic (CT) systems with the unidirectional disturbance inputs. The rectangular box indicates the elementary model of single compartment corticothalamic system. Excitatory (inhibitory) connections indicated with red arrows (purple buttons). The top arrow indicates the impulse or noise disturbance $d(t)$ to CT system I, whose output $y(t)$ (red arrow between the rectangular boxes) has an effect on CT system II, and our aim is to make $y(t)$ smaller and attenuate the effect on system II.

2.2. *Bistability dynamics*

Figure 1(a) shows that under the parameters given above the system is at background resting state. However, when applied a pulse stimulus on the system at 10 s, the system transits from a resting state to the SWD oscillations (see Figure 1(b)). We begin with the simplest of our scenarios. Figure 1(b) shows the maxima and minima of the model output for different values of the parameter h_{tc}. If h_{tc} take smaller negative values ($h_{tc} <\approx -2$, left side of Figure 1(a)), there is only one stable equilibrium solution, all simulations converge to the steady state (stable focus). For less negative values ($-2 <\approx h_{tc} < -1.5$, shaded area of Figure 1(b)), a bistable region exists between the stable focus and the SWD oscillations. This arises following a fold of cycles bifurcation at $h_{tc} \approx -2$. The schematic diagram of bistability can be seen from Figure 1(c). The purple and yellow regions are the attractors of the stable focus and SWD, respectively. The stable focus can be considered analogous to resting state background EEG, and the high amplitude oscillatory attractor to be the seizure state. Figure 1(a) illustrates that stimulus can drive the system out of the attractor of stable focus and into the attractor of SWD. In the bistable region, a separating manifold (separatrix) exists between the two states in four dimensional state space. This manifold is highly complex in structure [22]. Transitions between non-seizure and seizure states can occur when a stimulus beyond the separatrix occurs. Beyond the disappearance of the stable focus (due to a subcritical Hopf bifurcation) at h_{tc} > -1.5, monostable SWD and slow waves exist (right hand side of Figure 1(b)).

3. A network model with disturbance and the design of a preview control method

In this section, we propose a corticothalamic neural network model with disturbance and simultaneously design the corresponding preview control method which can suppress the epileptic seizure SWD dynamics. Figure 3 gives the configuration of serve systems with optimal preview control.

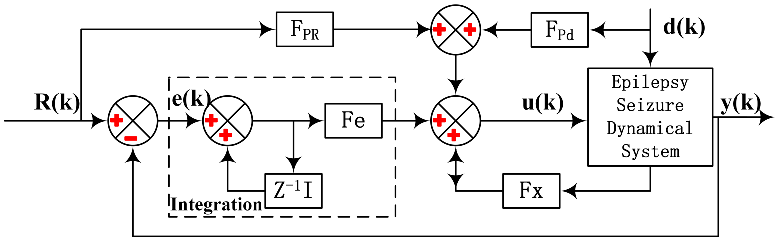

Figure 3. Configuration of serve systems with optimal preview control. $R(k)$, $e(k)$, $u(k)$, $d(k)$, and $y(k)$ are the reference signal, error signal, control input, disturbance signal and output signal of the system, respectively; and Fe, Fx, F_{PR}, and F_{Pd} are the error feedback, state feedback, feed-forward reference signal compensation, and feed-forward disturbance signal compensation of the system, respectively. $z^{-1}I$ is denoted as a transformation process that transforms the error of the $(k+1)^{th}$ step into the $e(k)$.

3.1. Control model with disturbance

Let

$$x(t) = (PY(t) \quad IN(t) \quad TC(t) \quad RE(t))^{\mathrm{T}}. \tag{3.1}$$

The time series of model output is defined as the mean value of PY and IN in variables:

$$y(t) = Cx(t), \tag{3.2}$$

where $C = (0.5 \quad 0.5 \quad 0 \quad 0)$.

Then, based on the (2.1), the CT model with both disturbance and control can be rewritten as

$$\begin{cases} \dot{x}(t) = A_0 x(t) + f_0(x(t)) + B_0 u(t) + D_0 d(t), \\ y(t) = Cx(t). \end{cases} \tag{3.3}$$

where

$$A_0 = \begin{pmatrix} -\tau_1 & 0 & 0 & 0 \\ 0 & -\tau_2 & 0 & 0 \\ 0 & 0 & -\tau_3 & -\tau_3 C_6 a \\ 0 & 0 & \tau_4 C_5 a & -\tau_4 - \tau_4 C_4 a \end{pmatrix}. \tag{3.4}$$

The control input of the system is

$$u(t) = (u_1(t) \quad u_2(t) \quad u_3(t) \quad u_4(t))^{\mathrm{T}} \tag{3.5}$$

and

$$B_0 = (B_1 \quad B_2 \quad B_3 \quad B_4) \tag{3.6}$$

is the control matrix of $u(t)$. Considering different control strategies inputs, the number of elements u_i in $u(t)$ is adjusted with the choice of strategy, while the number of B_i in B_0 is adjusted to be consistent with the number of u_i. B_i is a 4×1 column vector.

The exogenous disturbance to the system is denoted by

$$d(t) = \begin{pmatrix} d_1(t) & d_2(t) & d_3(t) & d_4(t) \end{pmatrix}^{\mathrm{T}}. \tag{3.7}$$

And the exogenous disturbance matrix is taken as

$$D_0 = \begin{pmatrix} 400 & 0 & 0 & 0 \\ 0 & 100 & 0 & 0 \\ 0 & 0 & 200 & 0 \\ 0 & 0 & 0 & 300 \end{pmatrix}. \tag{3.8}$$

The values in D_0 represent the influence degree of disturbance on this variable. The larger the value, the greater the influence of disturbance. This paper chooses the value that has a significant effect of simulation.

The nonlinear term of the (2.1) can be written as

$$f_0(x(t)) = \begin{pmatrix} \tau_1 h_{py} + \tau_1 C_1 S(x_1(k)) - \tau_1 C_3 S(x_2(k)) + \tau_1 C_9 S(x_3(k)) \\ \tau_2 h_{in} + \tau_2 C_2 S(x_1(k)) \\ \tau_3 h_{tc} - \tau_3 C_6 b + \tau_3 C_7 S(x_1(k)) \\ \tau_4 h_{re} - \tau_4 C_4 b + \tau_4 C_5 b + \tau_4 C_8 S(x_1(k)) \end{pmatrix}. \tag{3.9}$$

3.2. System discretization

First, the discretization of system (3.3) is carried out. When the sampling period is $\delta = 0.001\ ms$, the approximate discrete-time model is of the following form:

$$\begin{cases} x(k+1) = Ax(k) + f(x(k)) + Bu(k) + Dd(k), \\ y(k) = Cx(k). \end{cases} \tag{3.10}$$

where

$$A = \delta * A_0 + I; \quad B = B_0 * \delta; \quad D = D_0 * \delta; \quad f(x(t)) = \delta f_0(x(t)). \tag{3.11}$$

We take the reference signal $r(k)$ as the step signal in order to compare the action of the system when it is added to the controller, and the step value of $r(k)$ is considered the equilibrium value of the system output stabilization. Furthermore, the external disturbance $d(k)$ as the rectangular signal or random gaussian white noise. Since the preview controller can use known future information, the basic assumptions about the reference signal and the disturbance signal are required as follows:

Assumption 1 The preview length of the reference signal is M_r, which means that at time k, $r(k)$, $r(k+1)$, $r(k+2)$, ..., $r(k+M_r)$ are available. The future values of the reference signal after time $k+M_r$ are constant with $r(k+M_r)$, namely, $r(k+M_r+j) = r(k+M_r), j = 1, 2, 3, ...$

Assumption 2 The preview length of the exogenous disturbance is M_d, i.e., at time k, the values $d(k)$, $d(k+1)$, $d(k+2)$, ..., $d(k+M_d)$ are available. After time $k+M_d$, the future values of the exogenous disturbance are equal to $d(k+M_d)$, namely, $d(k+M_d+j) = d(k+M_d)$, $j = 1, 2, 3, ...$

The error signal $e(k)$ is defined as the difference between the output and reference signal, i.e.,

$$e(k) = y(k) - r(k). \tag{3.12}$$

The purpose of the preview controller designed is that the output $y(k)$ can track the reference signal $r(k)$, asymptotically. In particular, we also aim to observe the effects of preview controllers and non-preview controllers when attacked by the random disturbances.

3.3. Derivation of the augmented error system

We construct an augmented error system to transform the tracking problem of the original system into the regulation problem of the augmented error system and use the linear matrix inequality (*LMI*) technique to design a preview controller.

First, we introduce the first-order backward difference operator Δ:

$$\Delta x(k) = x(k) - x(k-1). \tag{3.13}$$

Applying the operator to both sides of (3.10) leads to

$$\begin{cases} \Delta x(k+1) = A\Delta x(k) + B\Delta u(k) + \Delta f_k + D\Delta d(k), \\ \Delta y(k) = C\Delta x(k), \end{cases} \tag{3.14}$$

where $\Delta f_k = f(x(k)) - f(x(k-1))$ is the difference of the nonlinearity. Then, applying the same operator on the error signal

$$\Delta e(k+1) = \Delta y(k+1) - \Delta r(k+1). \tag{3.15}$$

Furthermore, combining (3.14) and (3.15) , we get

$$e(k+1) = e(k) + CA\Delta x(k) + CB\Delta u(k) + C\Delta f_k + CD\Delta d(k) - \Delta r(k+1). \tag{3.16}$$

Combining the first equation of (3.14) and (3.16) yields

$$\tilde{x}(k+1) = \tilde{A}\tilde{x}(k) + \tilde{B}\Delta u(k) + G_f\Delta f_k + G_d\Delta d(k) + G_r\Delta r(k+1), \tag{3.17}$$

where

$$\tilde{x}(k) = \begin{pmatrix} e(k) \\ \Delta x(k) \end{pmatrix}, \tilde{A} = \begin{pmatrix} I & CA \\ 0 & A \end{pmatrix}, \tilde{B} = \begin{pmatrix} CB \\ B \end{pmatrix}, G_f = \begin{pmatrix} C \\ I \end{pmatrix}, G_d = \begin{pmatrix} CD \\ D \end{pmatrix}, G_r = \begin{pmatrix} -I \\ 0 \end{pmatrix}. \tag{3.18}$$

To introduce the preview information on reference signal and disturbance signal, we define new vectors:

$$x_r(k) = \begin{pmatrix} \Delta r(k) \\ \Delta r(k+1) \\ \vdots \\ \Delta r(k+M_r) \end{pmatrix}, \tag{3.19}$$

$$x_d(k) = \begin{pmatrix} \Delta d(k) \\ \Delta d(k+1) \\ \vdots \\ \Delta d(k+M_r) \end{pmatrix}. \tag{3.20}$$

From assumptions about the reference signal and the exogenous disturbance, it is easily seen that

$$x_r(k+1) = A_r x_r(k), \quad x_d(k+1) = A_d x_d(k). \tag{3.21}$$

where

$$A_r = \begin{pmatrix} 0 & I & 0 & \ldots & 0 \\ 0 & 0 & I & \ldots & 0 \\ \vdots & \vdots & \vdots & \ddots & \vdots \\ 0 & 0 & 0 & \ldots & I \\ 0 & 0 & 0 & \ldots & 0 \end{pmatrix}, \quad A_d = \begin{pmatrix} 0 & I & 0 & \ldots & 0 \\ 0 & 0 & I & \ldots & 0 \\ \vdots & \vdots & \vdots & \ddots & \vdots \\ 0 & 0 & 0 & \ldots & I \\ 0 & 0 & 0 & \ldots & 0 \end{pmatrix}. \tag{3.22}$$

Considering (3.17) and (3.21), we can obtain the augmented error system:

$$\bar{x}(k+1) = \bar{A}\bar{x}(k) + \bar{B}\Delta u(k) + F\Delta f_k \tag{3.23}$$

where

$$\bar{x}(k) = \begin{pmatrix} \tilde{x}(k) \\ x_r(k) \\ x_d(k) \end{pmatrix}, \bar{A} = \begin{pmatrix} \tilde{A} & \tilde{G}_r & \tilde{G}_d \\ 0 & A_r & 0 \\ 0 & 0 & A_d \end{pmatrix}, \bar{B} = \begin{pmatrix} \tilde{B} \\ 0 \\ 0 \end{pmatrix}, F = \begin{pmatrix} G_f \\ 0 \\ 0 \end{pmatrix}, \tag{3.24}$$

$$\tilde{G}_r = \begin{pmatrix} 0 & G_r & 0 & \ldots & 0 \end{pmatrix}, \tilde{G}_d = \begin{pmatrix} G_d & 0 & \ldots & 0 \end{pmatrix}. \tag{3.25}$$

3.4. Design of the preview controller

For (3.23), we design a state feedback

$$\Delta u(k) = K\bar{x}(k), \tag{3.26}$$

where K is a matrix to be determined. Substitute the controller into (3.23), we get

$$\bar{x}(k+1) = (\bar{A} + \bar{B}K)\bar{x}(k) + F\Delta f_k. \tag{3.27}$$

The following lemma is needed to analyze conditions for asymptotic stability of the closed-loop system (3.27).

Lemma [41] Supposing the Assumptions 1 and 2 hold, if there exist a positive definite matrix $P > 0$ and matrices N, M, R, and constant μ such that

$$\begin{pmatrix} P - M - M^T & 0 & (\bar{A}M + \bar{B}R)^{\mathrm{T}} & (\gamma\bar{F}M)^{\mathrm{T}} \\ 0 & \mu I - N - N^{\mathrm{T}} & (FN)^{\mathrm{T}} & 0 \\ \bar{A}M + \bar{B}R & FN & -P & 0 \\ \gamma\bar{F}M & 0 & 0 & -\mu I \end{pmatrix} < 0, \tag{3.28}$$

where $\bar{F} = \begin{pmatrix} 0 & I & 0 & 0 \end{pmatrix}$ represents the relationship between $\Delta x(k)$ and $\bar{x}(k)$, and γ is the Lipschitz constant, i.e., for any $x, x' \in \mathbf{R}^n$, the inequation

$$\| f(x) - f(x') \| \leq \gamma \| x - x' \| \tag{3.29}$$

holds, then the closed loop system (3.23) is asymptotically stable, where the state feedback gain matrix $K = RM^{-1}$.

By utilizing the MATLAB toolbox, the linear matrix inequality (LMI) (3.28) in Lemma can be resolved. According to $f(x(t))$ in (3.11), we can calculate the Lipschitz constant γ of $f(x(t))$. Subsequently, the feasible solution P, M, N, R can be obtained, which ensures the validity of the LMI (3.28). If (3.28) is feasible, then the state feedback controller is $K = RM^{-1}$ that ensures the asymptotic stability of the closed-loop system (3.27). K is divided as follows in accordance with the division of state variables in (3.18), (3.20), and (3.24), i.e.,

$$K = \begin{pmatrix} K_e & K_x & K_r(0) & K_r(1) & \dots & K_r(M_r) & K_d(0) & K_d(1) & \dots & K_d(M_d) \end{pmatrix}. \tag{3.30}$$

After substituting K into (3.26), we can get

$$\Delta u(k) = K_e e(k) + K_x \Delta x(k) + \sum_{i=0}^{M_r} K_r(i)\Delta r(k+i) + \sum_{i=0}^{M_d} K_d(i)\Delta d(k+i). \tag{3.31}$$

According to the definition of $\Delta u(k)$, the preview controller of system (3.10) can be taken as the following theorem.

Theorem If there exist a positive definite symmetric matrix M and a matrix N such that LMI (3.28) holds, and LMI (3.28) has a feasible solution, then the preview controller of system (3.10) is

$$\begin{aligned} u(k) = K_e \sum_{i=0}^{k} e(i) + K_x x(k) + \sum_{i=0}^{M_r} K_r(i) r(k+i) + \sum_{i=0}^{M_d} K_d(i) d(k+i) \\ - \sum_{i=0}^{M_r-1} K_r(i) r(i) - \sum_{i=0}^{M_d-1} K_d(i) d(i). \end{aligned}$$

Note that it is assumed that when $i < 0$, $x(i) = 0$, $u(i) = 0$, $r(i) = 0$. The coefficients in $u(k)$ are shown in (3.30). Under this controller, the output of the system (3.10) can asymptotically track target signal.

4. Simulation results

Epileptic phenomena are generally modeled by a bistability of silence and seizure-like bursting. The stimulation disturbance is often able to induce epileptic seizures which can also be affected by random factors such as noise in the seizure process. Our aim is to design a controller that can control the system to normal state. In particular, it can maintain system ability to prevent secondary seizures when the system is disturbed again.

Observed from the analysis above, a preview controller is obtained based on the corticothalamic network dynamic model capable of generating the spike and wave discharges (SWD) of idiopathic generalized epilepsy (IGE). In fact, the control problem of SWD is essentially the tracking problem of the closed-loop system for the normal state.

We use parameters which place the model in bistability state. Thus, the appropriate stimulation disturbance can induce the SWD seizures. Considering that SWD control of the normal state is essentially a problem of tracking the normal state, we take the reference signal as the following step function:

$$r(t) = \begin{cases} 0, & 0ms \le t < 2305ms, \\ 0.1755, & 2305ms \le t \le 5000ms. \end{cases} \tag{4.1}$$

We have assumed that the initial value of the state is $x(0) = (0.1724 \quad 0.1787 \quad -0.0818 \quad 0.2775)^T$. We select the initial values and then test that they are in the domain of attraction of the system stability. Moreover, we focus on the oscillatory case of the system and the case after being disturbed, which by its very nature is not affected by the initial values. Therefore, we do not provide an in-depth discussion of this detail. According to the system output value when the system is stable under this initial value, the tracking signal $r(k)$ takes on the value of 0.1755.

The exogenous disturbance $d_1(t) = d_2(t) = d_3(t) = d_4(t)$ is as follows

$$d_{1,2,3,4}(t) = \begin{cases} 0, & 0\ ms \leq t < 500\ ms \\ 0.1, & 500\ ms \leq t \leq 502\ ms \\ 0, & 502\ ms < t < 2850\ ms \\ 0.1, & 2850\ ms \leq t \leq 3000\ ms \\ 0, & 3000\ ms < t < 3150\ ms \\ -0.1, & 3150\ ms \leq t \leq 3300\ ms \\ 0, & 3300\ ms < t < 3700\ ms \\ normrnd(0, 0.02, 1, 1001), & 3700\ ms \leq t \leq 4700\ ms \\ 0, & t > 4700\ ms \end{cases} \tag{4.2}$$

We take values of impulses and white noise for disturbances and verify that they cause seizures without the controller.The simulation results are shown in Figure 4.

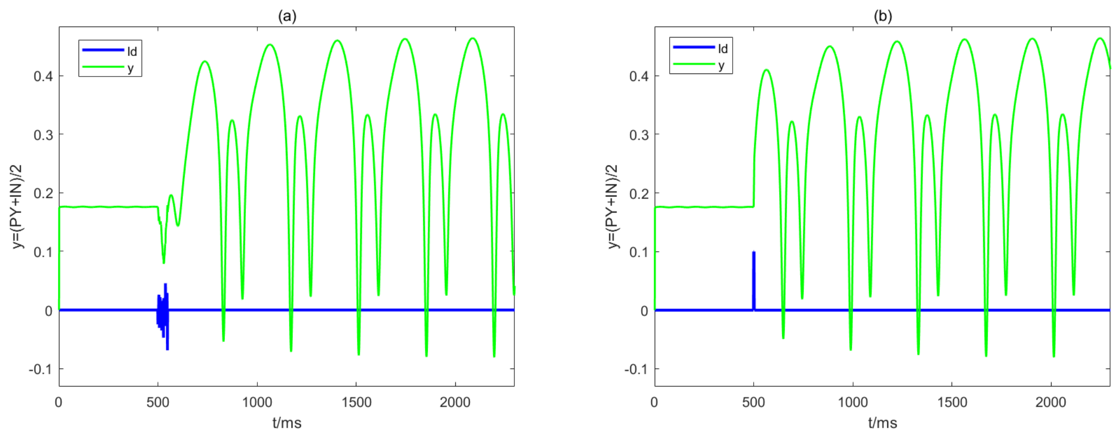

Figure 4. The blue line indicates (a) noise interference and (b) impulse interference, and the green line represents the system output. At $t = 500\ ms$, a noise stimulus $d(t) = normrnd(0, 0.02, 1, 50)$ and a pulsed stimulus of $d(t) = 0.1$ are added in the system, where *normrnd* represents a random number matrix of normal distribution with the mean of 0 and the standard deviation of 0.02 in the form of 1×50.

We obtain a time length of 2300 ms in Figure 4, during which the controller does not function. The results in Figure 4 demonstrate that our choice of interference is informative. To examine the difference before and after the controller takes effect, we will add the controller for the time period $t > 2300\ ms$ in following simulations.

Additionally, starting from the physical and actual meanings, we compared the effects of single-input controller and multiple-input controller on the model outputs while tracking the reference signal and receiving random disturbance. On this basis, we give some definitions of the coefficient matrix B of the controller $u(t)$ in system (3.10).

We take the dimension of B as $4 \times i$ (i = 1, 2, 3, 4), where i indicates the number of input channels, and we assume that each input channel can only affect one nucleus in the model (i.e., PY, IN, TC, RE). The element of B are 0 or 1, then if $B_{ji} = 1$ $(i, j = 1, 2, 3, 4)$, it means that the i^{th} input channel has an effect on the j^{th} nucleus. The number of element 1 is equal to i.

Moreover, in order to observe the effect of preview references and disturbances on the tracking performance, we choose a preview length with good results through many experimental simulations. Then, two cases are considered, separately: (i) $M_r = 0\ ms$, $M_d = 0\ ms$ (no preview); (ii) $M_r = 3\ ms$, $M_d = 3\ ms$.

4.1. Preview controller can completely abate the SWD discharges with effectively eliminating disturbance

From $t = 2300\ ms$ to $t = 5000\ ms$, the controller is applied to the system. We divide the simulation results into 4 groups according to the dimension of B and compare the effect of the controller with or without preview.

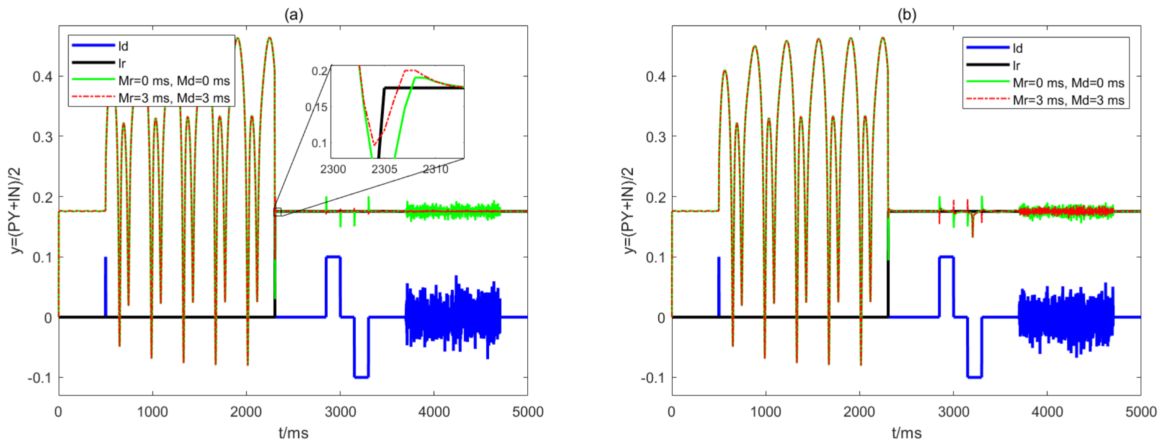

Figure 5. The controllers with one input channel applied on (a) (PY) and (b) (IN). The blue line and the black in figures represent the stimulus disturbance and reference signal to the corticothalamic dynamic system. The green line and red line represent the system output response of the non-preview controller and the preview controller, respectively. The effects of controllers with TC or RE input channel are not shown because these strategies cannot remain stability of system according to LMI (3.28).

In the period $0 \leq t < 500\ ms$, the system is in the non-epileptic seizure state. Then at time $t = 500\ ms$, the external disturbance $d(t) = 0.1$ leads to the seizure of the system, which is represented by the production of spike-wave discharges. After $t = 2300\ ms$, the controller starts to work and suppress seizures (i.e., track the reference signal). At this period, we apply a impulse disturbance

$d(t) = 0.1$ and $d(t) = -0.1$ to the system. Additionally, random factors such as noise can also induce seizures (Figure 4(a)). For example, input from subcortical to cortical. This hypothesis is supported by the dynamics of the thalamic-cortical circuit and mechanical computational models of SWD seizure duration statistics obtained from rat and human models. We simulate the noise in the time period $3700\ ms \leq t \leq 4700\ ms$. The random disturbance is $d(k) = normrnd(0, 0.02, 1, 1001)$.

As shown in the Figure 5 about controllers with only one input channel, although seizures both can be suppressed by controller with or without preview, the preview controller can effectively eliminate or reduce the effect of secondary disturbance on the system.

The local zoomed-in graph in Figure 5(a) shows that the preview controller can use the information from the future reference signal with a time length $M_r = 3\ ms$ to control the system outputs to react earlier. The preview controllers can make the system shift more gently than the non-preview controller which has a more drastic change in the system output. This may cause patient discomfort in clinical applications, which is another reason why we considered applying the preview controller to epilepsy seizures. Furthermore, we also utilize the future information of the disturbance signal with a length of $M_d = 3\ ms$. The effect graph is similar to the local zoomed-in graph in Figure 5. In order to make the images more concise, we do not draw local zoomed-in diagrams for the other simulation result diagrams.

We also show the results of the other strategies to compare the effects of preview and non-preview controllers in the following Figures 6–8.

The results show that the controllers (without preview and with preview) can effectively terminate the epileptic seizure at $t = 2300\ ms$, and when the system receives secondary disturbances (impulses and white noise), the preview controller(red line in the figures) can make the system oscillate less or even no oscillations. Comparing controller effects in different strategies, we can find that the effect of the controllers containing IN channel (the controllers without PY channel) are worse than the effect of other controllers with PY channel. We discuss PY and IN in terms of their physiological roles.

PY expresses excitatory neurons and IN indicates inhibitory neurons. The purpose of the controllers we designed is to regulate neurons. Based on the different physiological roles of PY and IN and the result of simulations, we speculate that PY has a greater role in influencing epileptic seizures combined with the knowledge we already know. Therefore, the controller is better able to keep the system in a stable state when it functions on the PY channel.

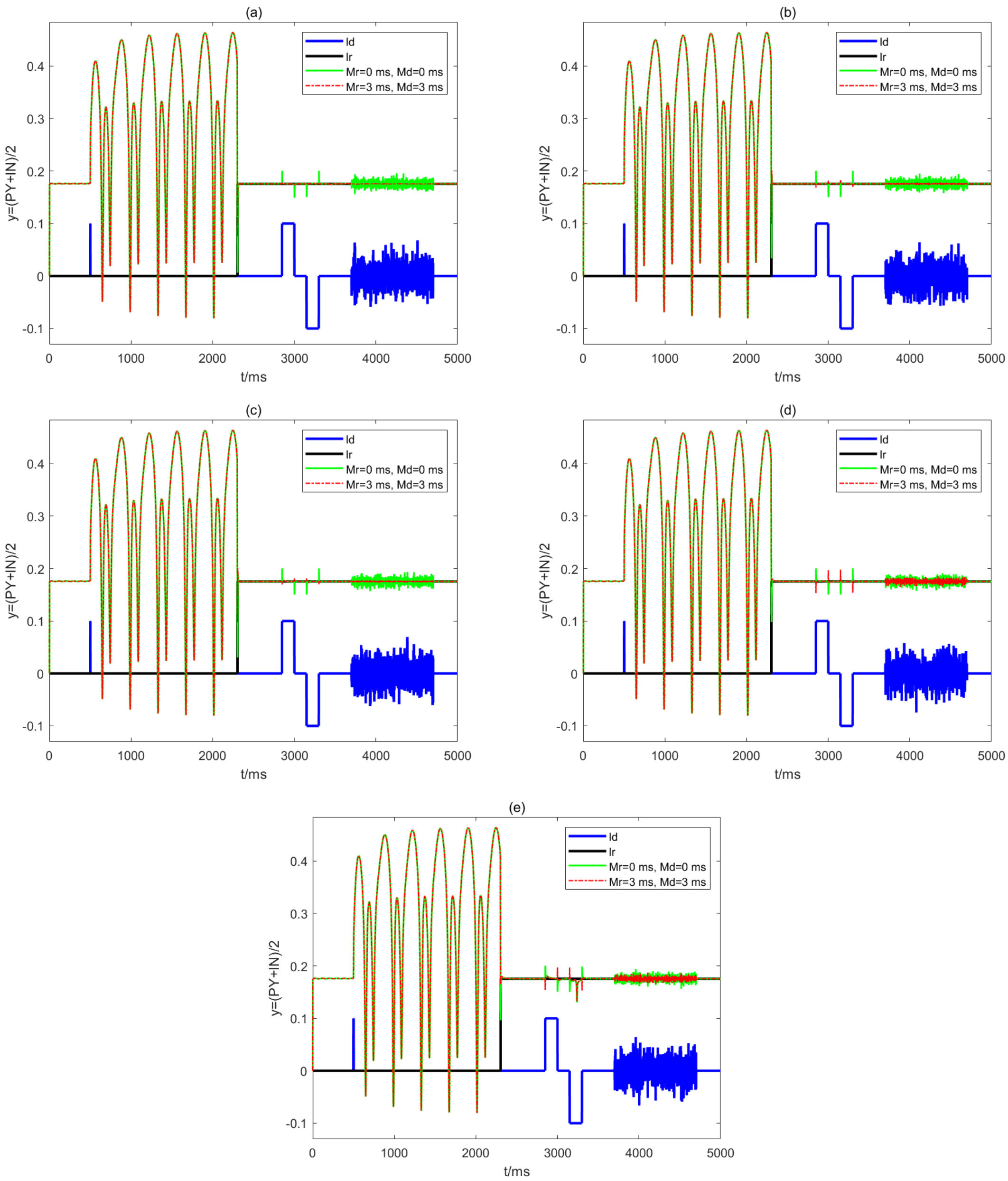

Figure 6. The controllers with two input channels applied on (a) (PY, IN), (b) (PY, TC), (c) (PY, RE), (d) (IN, TC), and (e) (IN, RE), respectively. Other explanations refer to the marks of Figure 5. According to the results of LMI (3.28), the effects of controllers with TC and RE input channel are not simulated because this strategy does not allow the system to remain asymptotically stable.

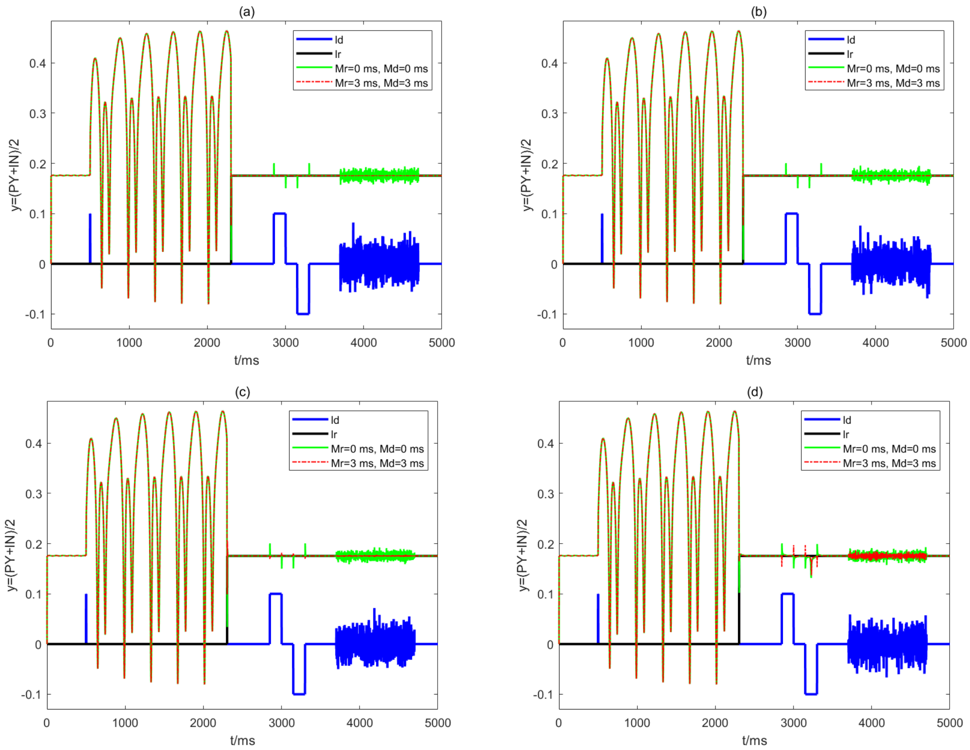

Figure 7. The controllers with three input channels applied on (a) (PY, IN, TC), (b) (PY, IN, RE), (c) (PY, TC, RE), and (d) (IN, TC, RE), respectively. Other explanations refer to the marks of Figure 5. Compared with the results in Figure 5, the controllers containing PY input channel stabilize the system well after adding an input channel to the controllers. In contrast, the controllers in (d) do not act on PY, at which point the oscillations occurring in the output of the system are significantly larger than in the previous three figures.

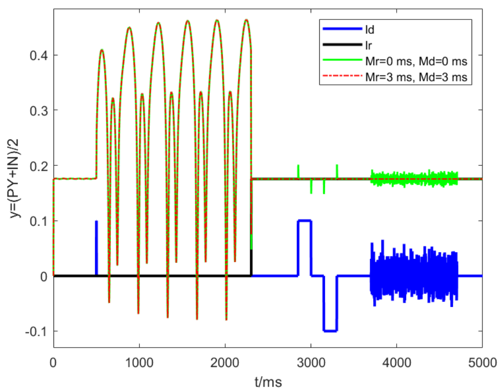

Figure 8. The controllers with four input channels applied on PY, IN, TC and RE. Other explanations refer to the caption of Figure 5. When the controllers function on all input channels, the advantage of the preview controller (red line) is obvious, as it allows the system to be balanced essentially and break away from disturbances.

4.2. Preview control can produces a lower performance consumption

Practically speaking, we would like the controllers to be effective in attenuating or terminating seizures while generating lower energy consumption, which would increase the feasibility of clinical applications. Therefore, we introduce a performance index function to evaluate the energy consumption of both preview controller and non-preview controller under different input control strategies. With minor modifications, we integrate our needs into the formula of the performance function J in [42]. We only consider the tracking performance of the system, i.e., the tracking error $e(k)$ and the consumption of input $u(t)$ are both as small as possible. The performance index function J for error system (3.10) is defined as

$$J = \sum_{k=1}^{\infty} [e^{\mathrm{T}}(k) Q_e e(k) + u^{\mathrm{T}}(k) Q_u u(k)], \tag{4.3}$$

where Q_e and Q_u are identity matrices of appropriate dimensions.

First, we compare the controller input values for different strategies. For inputs with many input channels, we compute the modulus length of $u(t)$, which is defined as

$$\| u(t) \| = \sqrt{\sum_{i=1}^{4} u_i^2}. \tag{4.4}$$

The input variation images for Figures 5–8 are provided in Figures 9–12.

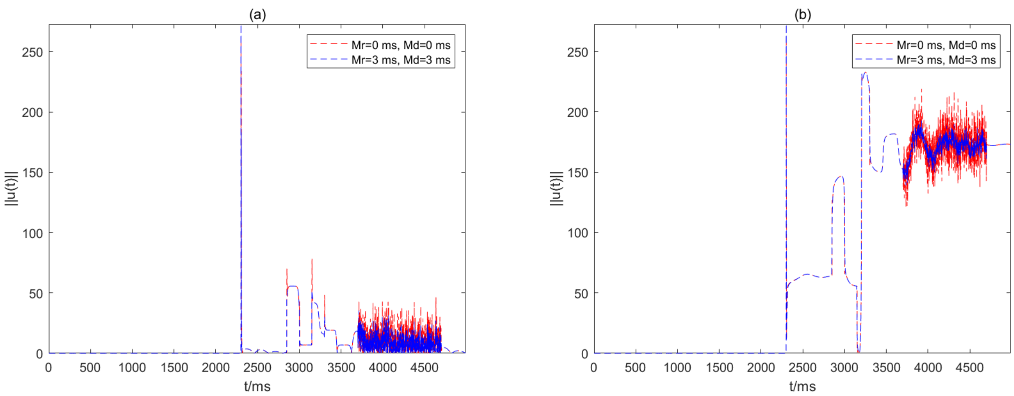

Figure 9. The control inputs with one input channel of (a) PY and (b) IN, respectively. The red and blue lines represent the inputs from non-preview controller and preview controller, respectively. Due to the differences in the input channels, the variations in the controller inputs are quite different, even though the trends in the system outputs remain consistent. It is evident that the controllers with IN input channel have larger input values.

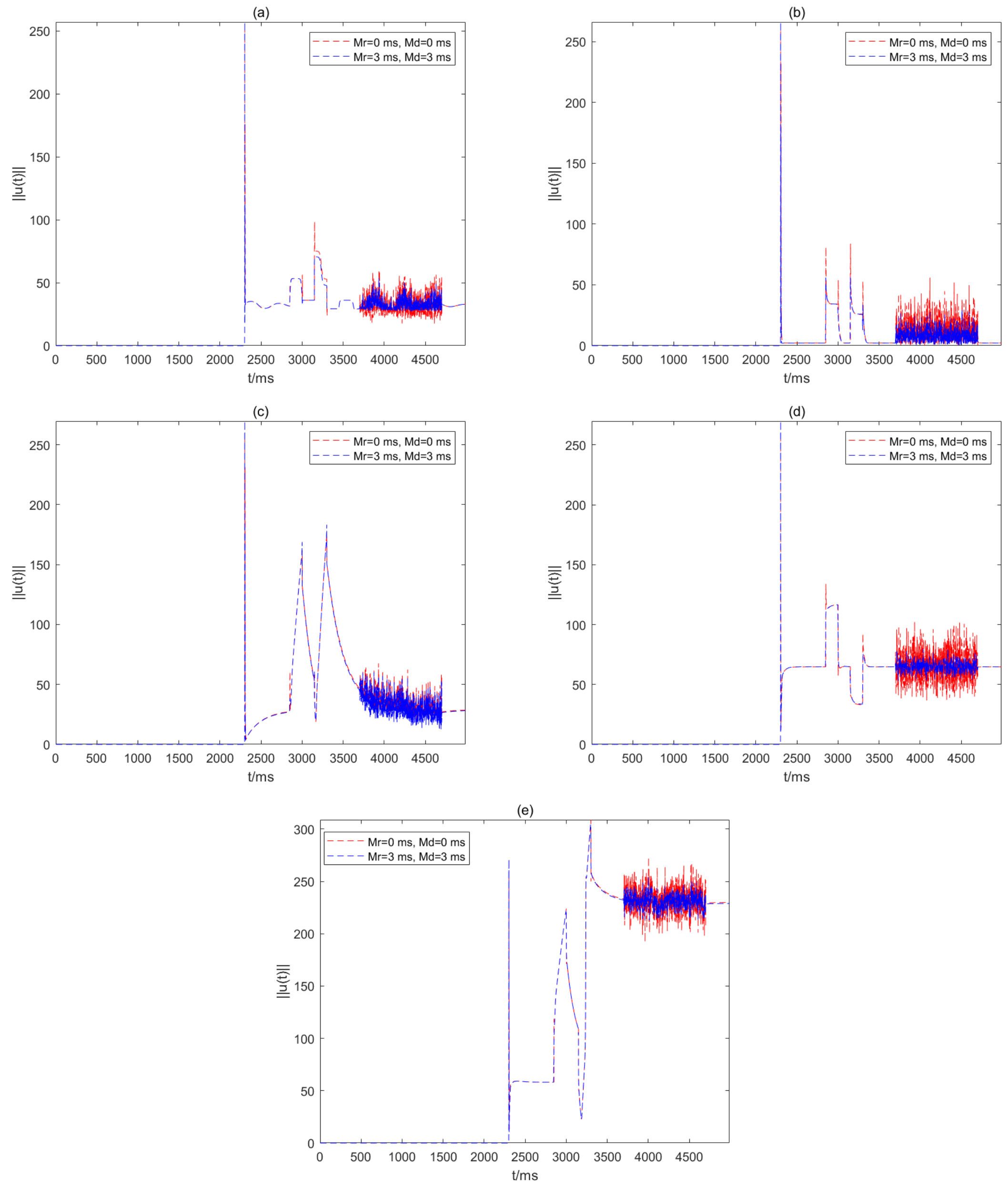

Figure 10. The control inputs with two input channels of (a) (PY, IN), (b) (PY, TC), (c) (PY, RE), (d) (IN, TC), and (e) (IN, RE), respectively. The red and blue lines represent the inputs from non-preview controller and preview controller, respectively. The addition of one input channel reduces the controller input values to some extent in the strategies associated with IN (i.e., (a) and (d)). In contrast, there is an increase of controller inputs in (e), which indicates that the RE input channel also produces a larger input value.

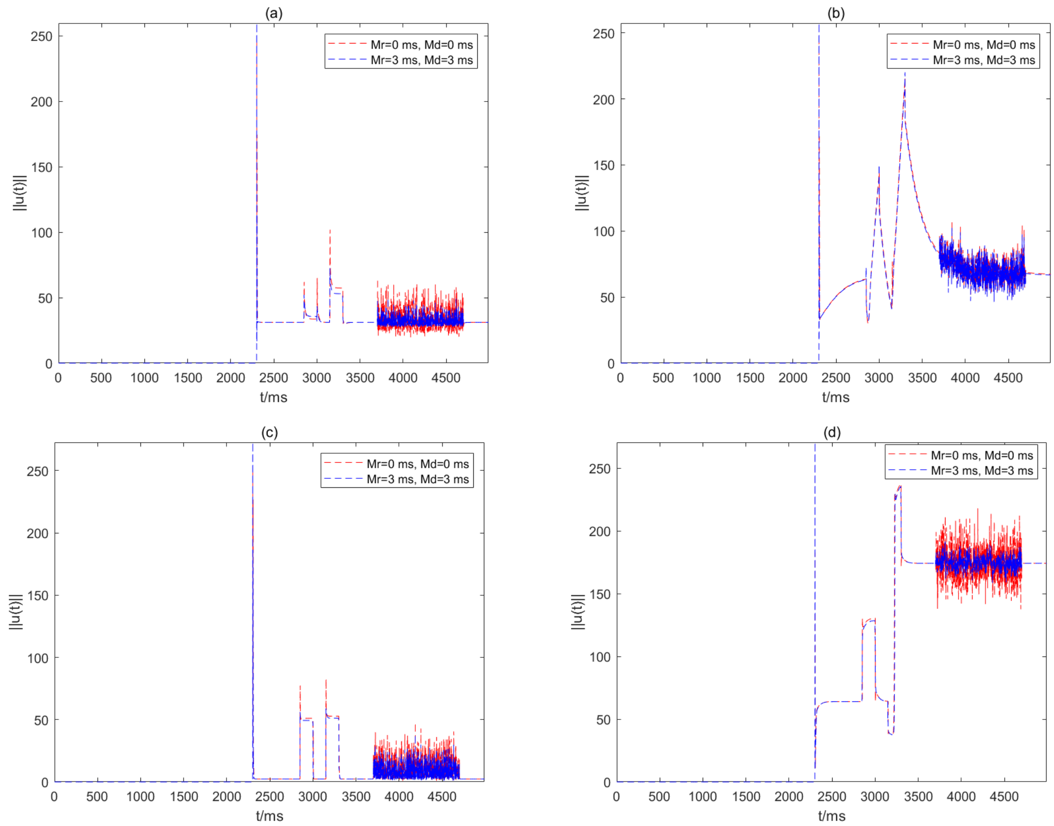

Figure 11. The control inputs with three input channels of (a) (PY, IN, TC), (b) (PY, IN, RE), (c) (PY, TC, RE), and (d) (IN, TC, RE), respectively. The red and blue lines represent the inputs from non-preview controller and preview controller, respectively. When the controller contains both IN and RE input channels, the fluctuation of the input values is significantly more drastic when the system receives a secondary impulse disturbance ($2850\ ms \leq t \leq 3000\ ms$ and $3150\ ms \leq t \leq 3300\ ms$).

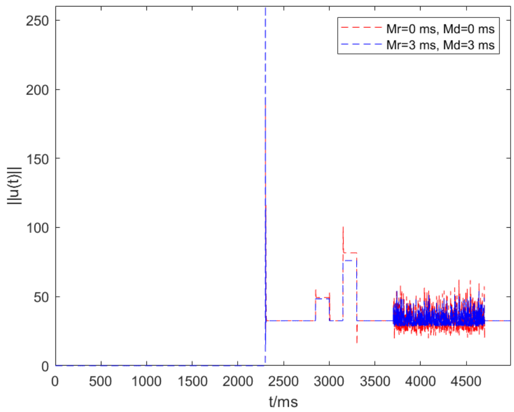

Figure 12. The control inputs with four input channels of (PY, IN, TC, RE). The red and blue lines represent the inputs from non-preview controller and preview controller, respectively. The maximum number of controller input channels has been reached, although there has been little rise in the controller input values.

We can tentatively draw a conclusion by comparing the controller input values for the different strategies described above. Depending on the number of input channels required, we can appropriately avoid IN and RE input channels, as they generate larger input values and thus higher consumption.

Then, we combine the partial statistics of the controller input values and the values of the performance function J to filter the controller strategies for low energy consumption. We display the data in Table 1 (without preview) and Table 2 (with preview). The statistics in the table are derived from he time period when the controllers function.

Table 1. Statistical list of non-preview controller with different input channels and J.

Input number	Position	Statistics Max_1	Max_2	Min	$Average$	J ($\times 10^5$)
1	PY	262.625	78.239*	0.002	12.047	5.1287
	IN	262.735	232.826	0.121	139.456	4.3053
2	PY, IN	251.913	98.477	18.040	36.070	3.2085*
	PY, TC	258.696	83.855	0.158	10.554*	6.3334
	PY, RE	259.704	175.852	4.183	48.334	5.1352
	IN, TC	256.170	133.848	33.061	66.005	5.6988
	IN, RE	258.851	308.916	22.800	183.68	5.1028
3	PY, IN, TC	250.183	101.933	19.177	34.184	5.0195
	PY, IN, RE	248.368	215.747	30.032	77.984	3.7227
	PY, TC, RE	253.297	82.721	0.758	12.325	5.5742
	IN, TC, RE	249.417	237.820	37.268	141.434	5.0440
4	ALL	189.853*	100.547	14.963	37.125	3.7425

* Minimum value in the current statistic (column)

Table 2. Statistical list of preview controller with different input channels and J.

Input number	Position	Statistics Max_1	Max_2	Min	$Average$	J ($\times 10^5$)
1	PY	272.775	55.665*	0.000	10.609	3.1495
	IN	274.649	232.811	0.117	139.342	1.3644*
2	PY, IN	257.139*	70.626	26.996	35.531	2.3799
	PY, TC	266.043	56.124	0.116	8.413*	3.4618
	PY, RE	269.767	183.325	3.195	47.035	3.7638
	IN, TC	269.857	116.582	33.449	65.809	1.7433
	IN, RE	271.023	304.436	22.573	183.000	2.2811
3	PY, IN, TC	259.791	72.498	27.671	33.422	3.1426
	PY, IN, RE	257.160	220.144	32.023	76.689	3.3524
	PY, TC, RE	272.795	58.995	0.802	10.734	3.9997
	IN, TC, RE	270.786	235.643	32.678	140.861	2.4181
4	ALL	260.263	76.000	28.454	36.568	3.6751

* Minimum value in the current statistic (column)

At time $t = 2300\ ms$, the controllers adjust and control the pathological signal to reach the normal reference state, which lead to the input increase greatly. $Max1$ indicates the maximum value of the input when the controllers start to work. However, we consider the preview length of the reference signal is M_r, the preview controller will use the future information with M_r length to adjust input value. Then, $Max1$ of preview controller is higher than the $Max1$ without preview. $Max2$ is the maximum value of input after reach the normal reference state for the first time. Min is the minimum value of input from $t = 2300$ to $t = 5000$ and $Average$ represents the average value during this period.

According to the data in the tables, we can find that the performance consumption J of the preview controller is significantly lower than that of the non-preview controller. Combining the analysis of the controller effects in Section 4.1 with the analysis of the controller input values and performance consumption, we can choose the preview controller strategy with PY and IN input channels. The performance consumption of this strategy is not the lowest, but it is the lowest compared to other strategies with great system output effects. Additionally, based on the conclusion of having large input values for the IN and RE channels, this strategy does not include both IN and RE channels. Moreover, in future practical clinical applications, the selected controller strategy must be modified to suit the situations of the individual patient. For example, is there a need to decrease the quantity of input channels, taking into account the potential effects of different channel numbers on the patient? Or is a lower system performance consumption needed to restore equilibrium?

5. Conclusions

In this paper, a preview controller is designed based on the methods of discretization, augmented error system and linear matrix inequality (LMI), using, as example, the corticothalamic network dynamic model capable of generating the generalized spike and wave discharges (SWD) of idiopathic generalized epilepsy (IGE).By comparing the effect of the action of the controllers designed and the performance function J, we obtained the following conclusions:

1) Compared to non-preview controllers, the preview controller enables the system to restore the equilibrium state, i.e., terminate the seizure, more quickly and gently; similarly, the preview controller enables the system to maintain smaller oscillations after the system receives a secondary disturbance. Combined with Figure 2, the preview controller can make the output $y(t)$ of CT system I has a lower impact on CT system II.

2) We discuss the controller input designed for different strategies. According to the output (3.2) of system, we analyze the advantages and disadvantages of the choice of strategies based on PY and IN neuronal nuclei from the perspectives of keeping system stability and performance consumption. Considering the possible negative effects of many input channels on the patient, we think that the preview controller with PY and IN input channels can provide both better control and lower consumption for clinical applications. The low consumption can reduce the loss of the controller in order to prolong the working time.

3) According to the data in Tables 1 and 2, the preview controller can produce overall lower performance consumption J. However, since the preview controller can utilize future information to make adjustments to the system at the current moment, it will have larger output values at individual moments, which is likely to cause physical discomfort to the patient. Therefore the preview length should not be selected too large and adjusted to a suitable length according to the actual needs.

To our knowledge, this is the first work investigating the preview control problem of epileptic seizures. This may be helpful to design clinically the robust and reliable seizure modulator.

Use of AI tools declaration

The authors declare they have not used Artificial Intelligence (AI) tools in the creation of this article.

Acknowledgments

This research was supported by the National Natural Science Foundation of China (Grants Nos. 12072021,12372061 and 12332004).

Conflict of interest

The authors declare that there are no conflicts of interest.

References

1. Y. Aghakhani, A. P. Bagshaw, C. G. Bénar, C. Hawco, F. Andermann, F. Dubeau, et al., fMRI activation during spike and wave discharges in idiopathic generalized epilepsy, *Brain*, **127** (2004), 1127–1144. https://doi.org/10.1093/brain/awh136

2. P. N. Taylor, G. Baier, A spatially extended model for macroscopic spike-wave discharges, *J. Comput. Neurosci.*, **31** (2011), 679–684. https://doi.org/10.1007/s10827-011-0332-1

3. J. G. Milton, Epilepsy as a dynamic disease: a tutorial of the past with an eye to the future, *Epilepsy Behav.*, **18** (2010), 33–34. https://doi.org/10.1016/j.yebeh.2010.03.002

4. F. H. L. da Silva, W. Blanes, S. N. Kalitzin, J. Parra, P. Suffczynski, D. N. Velis, Dynamical diseases of brain systems: different routes to epileptic seizures, *IEEE Trans. Biomed. Eng.*, **50** (2003), 540–548. https://doi.org/10.1109/TBME.2003.810703

5. F. H. L. da Silva, J. P. Pijn, W. J. Wadman, Dynamics of local neuronal networks: control parameters and state bifurcations in epileptogenesis, *Progr. Brain Res.*, **102** (1994), 359–370. https://doi.org/10.1016/S0079-6123(08)60552-X

6. M. C. Mackey, L. Glass, Oscillation and chaos in physiological control systems, *Science*, **197** (1977), 287–289. https://doi.org/10.1126/science.267326

7. L. Glass, M. C. Mackey, Pathological conditions resulting from instabilities in physiological control systems, *Ann. N. Y. Acad. Sci.*, **316** (1979), 214–235. https://doi.org/10.1111/j.1749-6632.1979.tb29471.x

8. Z. C. Yang, D. G. Fan, Q. Y. Wang, G. M. Luan, Sharp decrease in the Laplacian matrix rank of phase-space graphs: a potential biomarker in epilepsy, *Cognit. Neurodyn.*, **15** (2021), 649–659. https://doi.org/10.1007/s11571-020-09662-x

9. P. Gloor, Neurophysiological basis of generalized seizures termed centrocephalic, in *The Physiopathogenesis of the Epilepsies*, Springfield, (1969), 209–236. Available from: https://cir.nii.ac.jp/crid/1573950399116067840.

10. W. W. Lytton, Computer modeling of epilepsy, *Nat. Rev. Neurosci.*, **9** (2008), 626–637. https://doi.org/10.1038/nrn2416

11. I. Soltesz, K. Staley, *Computational Neuroscience in Epilepsy*, Academic Press, San Diego, 2008. https://doi.org/10.1016/B978-0-12-373649-9.X5001-7

12. H. R. Wilson, J. D. Cowan, Excitatory and inhibitory interactions in localized populations of model neurons, *Biophys. J.*, **12** (1972), 1–24. https://doi.org/10.1016/S0006-3495(72)86068-5

13. J. G. Milton, P. H. Chu, J. D. Cowan, Spiral waves in integrate-and-fire neural network, in *Advances in Neural Information Processing Systems*, **5** (1992), 1001–1006. Available from: https://proceedings.neurips.cc/paper_files/paper/1992/file/07a96b1f61097ccb54be14d6a47439b0-Paper.pdf.

14. S. A. Hou, D. G. Fan, Q. Y. Wang, Regulating absence seizures by tri-phase delay stimulation applied to globus pallidus internal, *Appl. Math. Mech.*, **43** (2022), 1399–1414. https://doi.org/10.1007/s10483-022-2896-7

15. R. P. Lesser, S. H. Kim, L. Beyderman, D. L. Miglioretti, W. R. Webber, M. Bare, et al., Brief bursts of pulse stimulation terminate afterdischarges caused by cortical stimulation, *Neurology*, **53** (1999), 1081–2073. https://doi.org/10.1212/WNL.53.9.2073

16. G. K. Motanedi, R. P. Lesser, D. L. Miglioretti, M. M. Yuko, B. Gordon, W. R. S. Webber, et al., Optimizing parameters for terminating cortical afterdischarges with pulse stimulation, *Epilepsia*, **43** (2002), 836–846. https://doi.org/10.1046/j.1528-1157.2002.24901.x

17. A. Ashourvan, S. Pequito, A. N. Khambhati, F. Mikhail, S. N. Baldassano, K. A. Davis, et al., Model-based design for seizure control by stimulation, *J. Neural Eng.*, **17** (2020), 836–846. https://doi.org/10.1088/1741-2552/ab7a4e

18. J. Guckenheimer, P. Holmes, *Nonlinear Oscillations, Dynamical Systems, and Bifurcations of Vector Fields*, Springer-Verlag, New York, 1983. https://doi.org/10.1007/978-1-4612-1140-2

19. S. H. Strogatz, *Nonlinear Dynamics and Chaos*, Addison-Wesley, New York, 1994. Available from: http://hdl.handle.net/1813/97.

20. H. S. Haghighi, A. H. Markazi, Control of epileptic seizures by electrical stimulation: a model-based study, *Biomed. Phys. Eng. Express*, **7** (2021), 065009. https://doi.org/10.1088/2057-1976/ac240d

21. P. Suffczynski, S. Kalitzin, F. H. L. da Silva, Dynamics of non-convulsive epileptic phenomena modeled by a bistable neuronal network, *Neuroscience*, **126** (2004), 467—484. https://doi.org/10.1016/j.neuroscience.2004.03.014

22. P. N. Taylor, Y. J. Wang, M. Goodfellow, J. Dauwels, F. Moeller, U. Stephani, et al., A computational study of stimulus driven epileptic seizure abatement, *PLoS One*, **9** (2014), e114316. https://doi.org/10.1371/journal.pone.0114316

23. M. Breakspear, J. A. Roberts, J. R. Terry, S. Rodrigues, N. Mahant, P. A. Robinson, A unifying explanation of primary generalized seizures through nonlinear brain modeling and bifurcation analysis, *Cereb. Cortex*, **16** (2006), 1296–1313. https://doi.org/10.1093/cercor/bhj072

24. M. Cetin, Model-based robust suppression of epileptic seizures without sensory measurements, *Cognit. Neurodyn.*, **14** (2020), 51–67. https://doi.org/10.1007/s11571-019-09555-8

25. D. G. Fan, L. Y. Zhang, Q. Y. Wang, Transition dynamics and adaptive synchronization of time-delay interconnected corticothalamic systems via nonlinear control, *Nonlinear Dyn.*, **94** (2018), 2807–2825. https://doi.org/10.1007/s11071-018-4526-1

26. M. A. Kramer, B. A. Lopour, H. E. Kirsch, A. J. Szeri, Bifurcation control of a seizing human cortex, *Phys. Rev. E: Stat. Nonlinear Biol. Soft Matter Phys.*, **73** (2006), 041928. https://doi.org/10.1103/PhysRevE.73.041928

27. P. N. Taylor, J. Thomas, N. Sinha, J. Dauwels, M. Kaiser, T. Thesen, et al., Optimal control based seizure abatement using patient derived connectivity, *Front. Neurosci.*, **9** (2015). https://doi.org/10.3389/fnins.2015.00202

28. O. Zakary, M. Rachik, I. Elmouki, On the analysis of a multi-regions discrete SIR epidemic model: an optimal control approach, *Int. J. Dyn. Control*, **5** (2017), 917–930. https://doi.org/10.1007/s40435-016-0233-2

29. E. H. Essoufi, A. Zafrar, Boundary optimal control of time-space SIR model with nonlinear Robin boundary condition, *Int. J. Dyn. Control*, **10** (2022), 1279–1290. https://doi.org/10.1007/s40435-021-00886-1

30. S. Mollah, S. Biswas, Optimal control for the complication of Type 2 diabetes: the role of awareness programs by media and treatment, *Int. J. Dynam. Control*, **11** (2023), 877–891. https://doi.org/10.1007/s40435-022-01013-4

31. N. Birla, A. Swarup, Optimal preview control: a review, *Optim. Control. Appl. Methods*, **36** (2015), 241–268. https://doi.org/10.1002/oca.2106

32. X. Yu, F. C. Liao, L. Li, New results on observer-based robust preview tracking control for Lipschitz nonlinear systems, *J. Vib. Control*, **27** (2020), 2081–2096. https://doi.org/10.1177/1077546320953650

33. A. Khalil, N. Fezans, Gust load alleviation for flexible aircraft using discrete-time preview control, *Aeronaut. J.*, **125** (2020), 341–364. https://doi.org/10.1017/aer.2020.85

34. L. Li, F. C. Liao, Design of a preview controller for discrete-time systems based on LMI, *Math. Probl. Eng.*, **2015** (2015), 179126. https://doi.org/10.1155/2015/179126

35. E. Sitnikova, Thalamo-cortical mechanisms of sleep spindles and spike–wave discharges in rat model of absence epilepsy (a review), *Epilepsy Res.*, **89** (2010), 17–26. https://doi.org/10.1016/j.eplepsyres.2009.09.005

36. B. M. Bouwman, P. Suffczynski, F. H. L. da Silva, E. Maris, C. V. van Rijn, GABAergic mechanisms in absence epilepsy: a computational model of absence epilepsy simulating spike and wave discharges after vigabatrin in WAG/Rij rats, *Eur. J. Neurosci.*, **25** (2007), 2783–2790. https://doi.org/10.1111/j.1460-9568.2007.05533.x

37. J. C. Young, A. Paolini, M. Pedersen, G. Jackson, Genetic absence epilepsy: effective connectivity from piriform cortex to mediodorsal thalamus, *Epilepsy Behav.*, **97** (2019), 219–228. https://doi.org/10.1016/j.yebeh.2019.05.042

38. F. Marten, S. Rodrigues, P. Suffczynski, M. Richardson, J. R. Terry, Derivation and analysis of an ordinary differential equation mean-field model for studying clinically recorded epilepsy dynamics, *Phys. Rev. E: Stat. Nonlinear Biol. Soft Matter Phys.*, **79** (2009), 021911. https://doi.org/10.1103/PHYSREVE.79.021911

39. Y. J. Wang, M. Goodfellow, P. N. Taylor, G. Baier, Phase space approach for modeling of epileptic dynamics, *Phys. Rev. E: Stat. Nonlinear Biol. Soft Matter Phys.*, **85** (2012), 061918. https://doi.org/10.1103/PHYSREVE.85.061918

40. P. N. Taylor, M. Goodfellow, Y. J. Wang, G. Baier, Towards a large-scale model of patient-specific epileptic spike-wave discharges, *Biol. Cybern.*, **107** (2013), 83–94. https://doi.org/10.1007/s00422-012-0534-2

41. X. Yu, *Preview Control for Several Classes of Nonlinear Systems (in Chinese)*, Ph.D thesis, University of Science and Technology Beijing, 2019.

42. T. E. T. Tsuchiya, F. C. Liao, *The Latest Automatic Control Technology - Digital Preview and Predictive Control*, Beijing Science and Technology Press, Beijing, 1994.